

room temperature. Also, we calculated  $g$ -values for these crystals and compared them with the experimental results.

The measurements were made by the usual standing wave method. The crystal structure of  $\text{CuCl}_2 \cdot 2\text{H}_2\text{O}$  is orthorhombic, while the other two are tetragonal. The unit cell of these crystals contains two molecules. In the case of copper chloride, one of the molecules is derived from the other by a translation from the point  $(0, 0, 0)$  to  $(\frac{1}{2}, \frac{1}{2}, 0)$  followed by a reflection in the  $b$ - $c$  plane. In the case of potassium and ammonium salts, one is derived from the other by a translation from the point  $(0, 0, 0)$  to  $(\frac{1}{2}, \frac{1}{2}, \frac{1}{2})$  followed by a reflection in the  $(1, 0, 0)$  plane. Therefore, one may generally expect two resonance peaks. Actually, however, we obtained only one resonance maximum for all directions of the static magnetic field, which means that exchange coupling between copper ions is sufficiently strong that one resonance maximum occurs at the arithmetical mean of the two expected resonance fields.

Angular dependences of  $g$ -values and half-width values obtained experimentally for copper chloride and for the potassium salt are

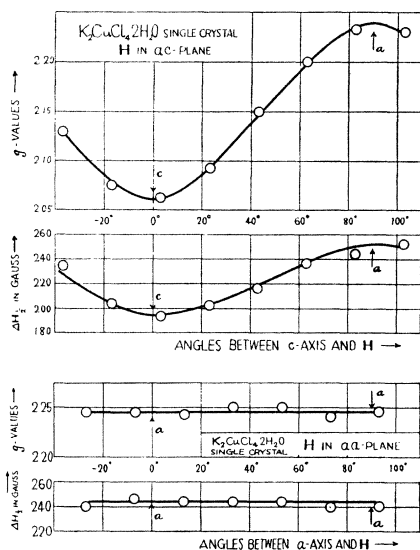


FIG. 2. Variation of  $g$ -values and half-widths ( $\Delta H_{1/2}$ ) with angle between the static field  $\mathbf{H}$  and the crystal axis in  $\text{K}_2\text{CuCl}_4 \cdot 2\text{H}_2\text{O}$ , at 3100 Mc/sec. Figures indicate these angular dependences for the cases in which  $\mathbf{H}$  rotates about the  $a$  axis and the  $c$  axis, respectively.

shown in Fig. 1 and Fig. 2. Those for the ammonium salt are almost the same as those for the potassium salt.

Since in these crystals the crystalline electric field at the position of the copper ion is of rhombic symmetry, we extended the calculation of Polder,<sup>2</sup> who treated the case of a tetragonal field, to the case of a rhombic field. Also, we have calculated self-consistent values for the induced moments of water molecules and chlorine ions; and then the expansion coefficients of the crystalline field at the position of copper ions were computed up to the fourth-order terms. Here, we assumed each ion or each water molecule to be a point charge and/or a point dipole at the position predicted by the

TABLE I. Calculated and experimental  $g$ -values.

	$\text{CuCl}_2 \cdot 2\text{H}_2\text{O}$		$\text{K}_2\text{CuCl}_4 \cdot 2\text{H}_2\text{O}$		$(\text{NH}_4)_2\text{CuCl}_4 \cdot 2\text{H}_2\text{O}$	
	Exp.	Calc.	Exp.	Calc.	Exp.	Calc.
$g_a^*$	2.195	2.248		2.290		2.122
$(g_a + g_b)/2$			2.24	2.28	2.25	2.23
$g_b^*$	2.075	2.052		2.278		2.336
$g_c$	2.26	2.278	2.06	2.04	2.05	2.01

\*  $g_a$  and  $g_b$  for the potassium and ammonium salts mean the  $g$ -values for the molecule at  $(0, 0, 0)$  in the direction  $(1, 1, 0)$  and  $(1, 1, 0)$ , respectively.

$x$ -ray analysis of Harker<sup>3</sup> and Chrobak.<sup>4</sup> The  $g$ -values thus calculated, and also the experimental  $g$ -values, are shown in Table I. As mentioned above, by the effect of exchange coupling, only the value  $\frac{1}{2}(g_a + g_b)$  can be obtained experimentally for the potassium and ammonium salts; these values are shown also in the table. The agreement is satisfactory for all of these salts.

The shapes of the absorption curves are not gaussian, but lie between gaussian and Lorentz-type absorption curves. Those for the potassium and ammonium salts almost coincide with the latter. Therefore, the experimental half-width  $\Delta H_{1/2}$  may not be compared directly with the theoretical value of  $(\langle \Delta H^2 \rangle_{AV})^{1/2}$  calculated by Van Vleck's formula.<sup>5</sup>  $\Delta H_{1/2}$  is much smaller than  $2.36 (\langle \Delta H^2 \rangle_{AV})^{1/2}$ , which corresponds to the theoretical half-width in the case of a gaussian-type absorption curve. Moreover, the angular dependence of  $(\langle \Delta H^2 \rangle_{AV})^{1/2}$  is not similar to the experimental results. The width for copper chloride is still narrower than that for copper sulfate pentahydrate, suggesting still stronger exchange coupling.

The details of the experiment and the calculations will be published elsewhere.

<sup>1</sup> These single crystals were made available by the courtesy of Dr. R. Kiriya of the Department of Chemistry, to whom we express our gratitude.

<sup>2</sup> D. Polder, *Physica* **9**, 709 (1942).

<sup>3</sup> D. Harker, *Z. Krist.* **93**, 136 (1936).

<sup>4</sup> L. Chrobak, *Z. Krist.* **88**, 35 (1934).

<sup>5</sup> J. H. Van Vleck, *Phys. Rev.* **74**, 1168 (1948).

## Production of Neutral Mesons by $\gamma$ -Rays Incident on Hydrogen\*

A. SILVERMAN AND M. STEARNS  
Cornell University, Ithaca, New York  
(Received July 5, 1951)

THE reaction  $\gamma + \text{H}^1 \rightarrow \pi^0 + \text{H}^1$  has been investigated by bombarding thin polyethylene and carbon targets with bremsstrahlung radiation from the 310-Mev Cornell synchrotron. The experimental arrangement is shown schematically in Fig. 1.

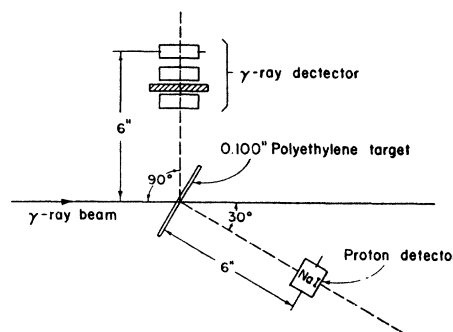


FIG. 1. Experimental arrangement (schematic).

The reaction is observed by detecting coincidences between the recoil proton and one of the decay  $\gamma$ -rays from the neutral meson. The energy and angle of the recoil proton are measured, and these two quantities, combined with the conservation equations, uniquely determine the energy of the incident  $\gamma$ -ray and the energy and angle of the neutral meson. In this manner it is possible to get the cross section for the production of neutral mesons as a function of  $\gamma$ -ray energy despite the continuous spectrum of the incident radiation. The technique of detecting the two decay  $\gamma$ -rays used by Steinberger, Panofsky, and Steller<sup>1</sup> does not give the meson energy directly, since a measurement of the angle between the two  $\gamma$ -rays does not uniquely determine the meson energy.

The  $\gamma$ -ray counter is similar to one described by Steinberger, Panofsky, and Steller<sup>1</sup> and is placed in the direction of the neutral meson for maximum efficiency. The proton counter is a thick NaI crystal in which the recoil proton comes to rest. The pulse height is thus a measure of the proton energy.

Most of the runs were taken with the proton counter at  $30^\circ \pm 3^\circ$  to the beam as shown in Fig. 1. For incident  $\gamma$ -rays between 200 and 310 Mev the corresponding neutral meson angle is  $90^\circ \pm 10^\circ$ . The  $\gamma$ -ray counter was correspondingly set at  $90^\circ$  (Fig. 1) with an angular aperture of  $\pm 5^\circ$ .<sup>2</sup> The hydrogen target was  $0.23 \text{ g/cm}^2$  slab of polyethylene and the carbon background was determined by making additional runs with a carbon target of equal stopping power for protons. The carbon background constituted about 22 percent of the total counts, varying from 10 percent in the highest energy interval to about 40 percent in the lowest. Accidentals were less than 5 percent and were measured directly by recording coincidences between the two counters with one channel delayed by more than twice the resolving time of the system.

Several auxiliary experiments were performed to check that the coincidences observed were due to the above reaction. These included studying the effect of removing the lead converter in the  $\gamma$ -ray counter, the change in counting rate as a function of the angle of the  $\gamma$ -ray detector, and the change in maximum energy of the recoil protons as a function of the angle of the proton counter.

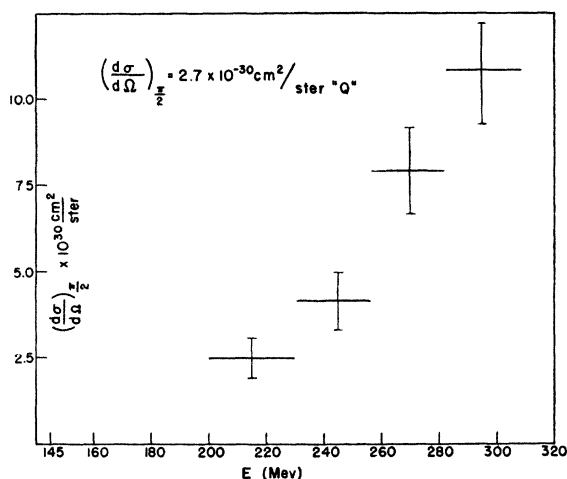


FIG. 2. Cross section for neutral meson production at  $90^\circ$  in the laboratory system as a function of incident  $\gamma$ -ray energy.

In each case the results were consistent with the production of neutral mesons from hydrogen. A more detailed description and quantitative results of these experiments will be published in a later paper.

The cross section for neutral meson production at  $90^\circ$  in the laboratory system as a function of the incident  $\gamma$ -ray energy is shown in Fig. 2. The indicated errors include estimated instrumental as well as statistical errors. The curve can be fitted with the power law  $d\sigma/d\Omega = k(E_\gamma - \mu c^2)^{1.8 \pm 0.5}$ , where  $E_\gamma$  is the incident  $\gamma$ -ray energy and  $\mu c^2$  the rest mass of the neutral meson. The curvature is in sharp contrast with that of the equivalent cross section for  $\pi^+$  mesons which approximates a one-half power law.<sup>3</sup> The absolute magnitudes of the two cross sections are roughly the same at 300 Mev.

A run was taken with the proton counter at  $45^\circ$ . The range of proton energies measured at this angle corresponds to  $\gamma$ -rays between 250 and 310 Mev. For these energies the corresponding neutral meson laboratory angle is  $60^\circ \pm 10^\circ$ . The ratio of the differential cross sections at  $60^\circ$  and  $90^\circ$  (laboratory angles) for 250–310-Mev incident  $\gamma$ -rays is  $(d\sigma/d\Omega)_{60^\circ}/(d\sigma/d\Omega)_{90^\circ} = 1.50 \pm 0.25$ . In the center-of-mass system the corresponding ratio becomes  $(d\sigma/d\Omega)_{76^\circ}/(d\sigma/d\Omega)_{112^\circ} = 1.10 \pm 0.20$ .

Attempts have been made to calculate these cross sections using both weak and strong coupling theories. The weak coupling approximation seems to give results in disagreement with the experimental results.<sup>4</sup> Brueckner and Case,<sup>5</sup> using a strong coupling theory involving an excited state of the nucleon, calculate results which seem to be in good agreement with the experimental ones.

\* This work was done under an ONR contract.

<sup>1</sup> Steinberger, Panofsky, and Steller, Phys. Rev. **78**, 802 (1950).

<sup>2</sup> The proton Compton scattering cannot contribute, since for protons scattered at  $30^\circ$  the  $\gamma$ -ray is scattered at approximately  $110^\circ$ .

<sup>3</sup> Bishop, Steinberger, and Cook, Phys. Rev. **80**, 291 (1950).

<sup>4</sup> M. F. Kaplon, Phys. Rev. **83**, 712 (1951).

<sup>5</sup> K. A. Brueckner and K. M. Case, Phys. Rev. (to be published).

## The Room Temperature Solubility of Iron in Copper

T. S. HUTCHISON AND JAMES REEKIE

Department of Physics, Royal Military College of Canada,  
Kingston, Ontario, Canada

(Received June 18, 1951)

THE room temperature solubility limit of iron in copper was determined some years ago by Hanson and Ford<sup>1</sup> and stated to be about 0.2 percent by weight. Other workers have suggested that the solubility is exceedingly small at room temperature,<sup>2</sup> while recent results,<sup>3</sup> concerned primarily with the effect of internal strain in copper-iron alloys, have tended to confirm the work of Hanson and Ford. We have reinvestigated this point by making direct measurements, at room temperature, of the density and of the lattice parameter of a number of copper-iron alloys containing up to 1.4 percent iron.

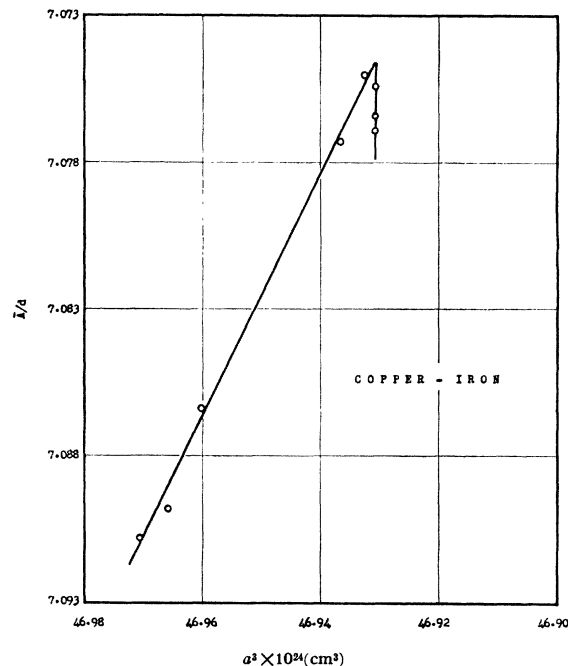


FIG. 1. Graph of  $\bar{A}/d$  vs  $a^2$  which shows a continuous linear variation of  $(\bar{A}/d)$  with  $a^2$  up to a solubility limit of 0.26 percent by weight of iron.

The specimens, in the form of rods about 3 mm in diameter and 15 cm long, were originally vacuum annealed for 10 hours at  $900^\circ\text{C}$  and then furnace cooled to  $25^\circ\text{C}$  over a period of about 10 hours. Density measurements were then made by weighing the rods in air and in water under closely controlled temperature conditions, making all necessary corrections, to obtain values which are considered accurate to about 1 part in 5000.